Mobile robot kinematic reconfigurability for rough-terrain

Karl Iagnemma[a], Adam Rzepniewski[a], Steven Dubowsky[a]*,
Paolo Pirjanian[b], Terrence Huntsberger[b], Paul Schenker[b]

[a]Department of Mechanical Engineering, Massachusetts Institute of Technology
Cambridge, MA 02139 USA

[b]Science and Technology Development Section, Jet Propulsion Laboratory,
California Institute of Technology, Pasadena, CA 91109 USA

ABSTRACT

Future planetary exploration missions will use rovers to perform tasks in rough terrain. Working in such conditions, a rover could become trapped due to loss of wheel traction, or even tip over. The Jet Propulsion Laboratory has developed a new rover with the ability to reconfigure its structure to improve tipover stability and ground traction. This paper presents a method to control this reconfigurability to enhance system tipover stability. A stability metric is defined and optimized on-line using a quasi-static model. Simulation and experimental results for the Sample Return Rover (SRR) are presented. The method is shown to be practical and yields significantly improved stability in rough terrain.

Keywords: Mobile robots, reconfigurability, static stability, rough terrain

1. INTRODUCTION

Mobile robots are increasingly being used in high-risk, rough terrain situations, such as planetary exploration[1]. Future planetary exploration missions will require mobile robots to perform difficult mobility tasks in rough terrain[2,3]. Such tasks can result in loss of vehicle stability, leading to tipover, and loss of wheel traction, leading to entrapment. Clearly, tipover instability can result in rover damage and total mission failure.

The Jet Propulsion Laboratory's Sample Return Rover (SRR) has been developed with the ability to actively modify its kinematic configuration to enhance rough terrain mobility[4]. Reconfigurable robots can reposition their center of mass to improve stability in rough terrain. For example, when traversing an incline the SRR can lower one side of its suspension to increase its stability margin, see Figure 1. It accomplishes this using two active shoulder joints that adjust the two angles q_1 and q_2, see Figures 1 and 2. It can also redistribute its center of mass by repositioning its manipulator. Both of these effects can be exploited to improve system stability.

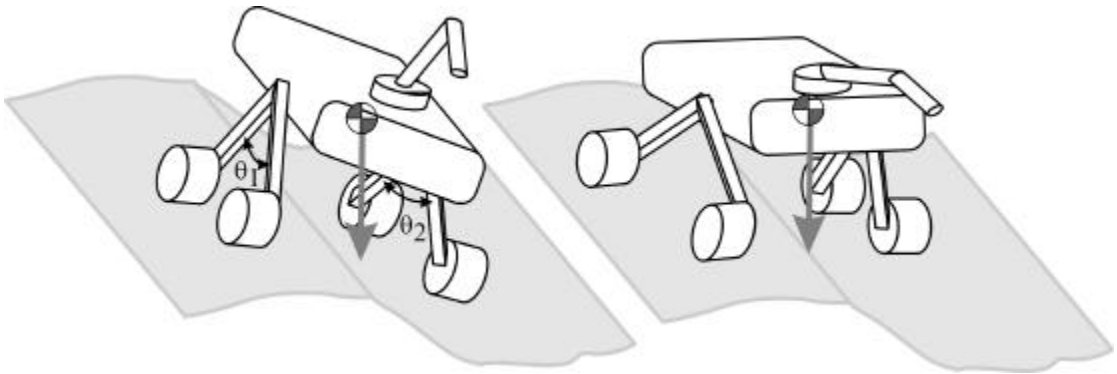

Figure 1. Example of reconfigurable robot improving rough-terrain stability by adjusting shoulder joints

* Correspondence: dubowsky@mit.edu

Previous researchers have suggested the use of kinematic reconfigurability to enhance rough-terrain mobility[5,6,7]. However, its practical effectiveness has not yet been demonstrated on a real rover system in rough terrain. In this paper a method for stability-based kinematic reconfigurability is presented, and applied to the JPL SRR[4]. Kinematic equations relating the reconfigurable joint variables to a vehicle stability measure are written in closed form. A performance index is defined based on this stability measure and a function that maintains adequate ground clearance, an important consideration in rough terrain. A rapid conjugate-gradient optimization of the performance index is performed subject to vehicle kinematic constraints. The method does not rely on a detailed map of the terrain. This prohibits a global optimization. However, wheel-terrain contact angles are estimated using simple on-board sensors[8,9]. This allows for local optimization. The method considers gravitational forces due to rover weight and can account for forces due to manipulation of the environment.

Computational requirements are light, being compatible with limited on-board resources of planetary rovers. Simulation and experimental results under field conditions show that kinematic reconfigurability can greatly improve rover stability in rough terrain.

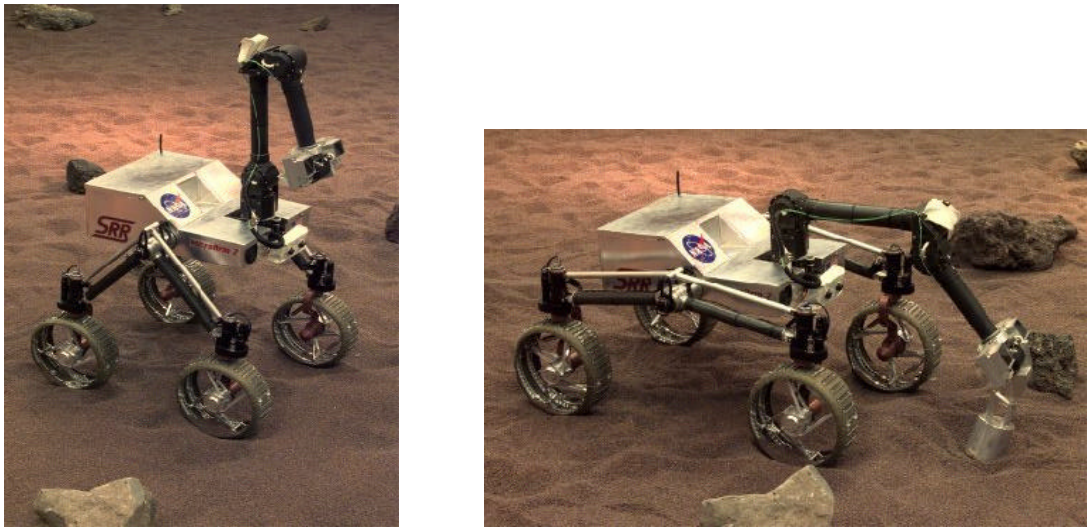

Figure 2. Jet Propulsion Laboratory Sample Return Rover (SRR)

2. GENERAL KINEMATIC RECONFIGURABILITY

Consider a general n-link tree-structured mobile robot on uneven terrain. An example of such a robot is shown in Figure 3. The n links can form hybrid serial-parallel kinematic chains. We assume the joints are active revolute or prismatic joints, and their values are denoted q_i, $i=\{1,\ldots,n\}$. We also assume the wheels or legs make point contact with the terrain. The m link-terrain contact points are denoted P_j, with their location defined as a vector $\mathbf{p}_j$ from the vehicle center of mass. The corresponding link-terrain contact angles are denoted a_j, $j=\{1,\ldots,m\}$.

The goal of kinematic reconfigurability is to improve robot performance by modifying the robot joint variables q_i to optimize a user-specified performance index. Such performance indices include static stability, wheel (or foot) traction, vehicle pose for optimal force application, and others. Since forward and inverse kinematic solutions of hybrid serial-parallel chains are in general difficult to formulate, analytical solutions often cannot be obtained for the optimal kinematic configuration. This motivates the use of numerical optimization techniques.

On-line kinematic reconfigurability requires three steps:

1) Evaluation of the robot kinematic configuration using on-board sensor readings. The configuration is defined as $Q = (q_1 \ldots q_n, a_1 \ldots a_m, f, c)$ where f and c denote the roll and pitch, respectively, of a reference member such as the vehicle body. The link (or wheel)-terrain contact angles a_j can be estimated from stereo range data or through kinematic methods[8,9].
2) Computation of a kinematic configuration Q which optimizes a performance index based on the joint variables q_i.
3) Motion from the current robot configuration Q to the optimal configuration Q .

Kinematic reconfigurability is divided here into two cases: internal reconfigurability and external reconfigurability. These cases are discussed below.

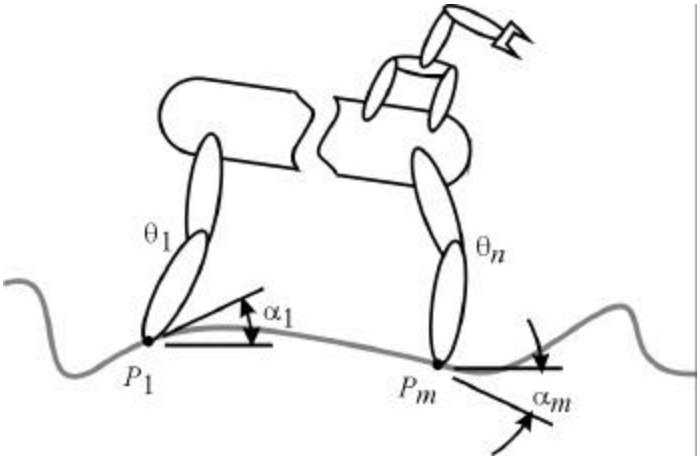

Figure 3. A general tree-structured robotic mechanism

2.1 Internal reconfigurability

In internal reconfigurability the link-terrain contact points P_j remain fixed relative to the terrain during the reconfiguration process, see Figure 4. For a wheeled robot, the wheels must be actively controlled to remain fixed without rolling. An internally reconfigurable robot has mobility greater than or equal to one while stationary on the ground (i.e. the robot has available self-motions), as defined by the Grubler mobility criterion[10]:

$$F = 6(l - j - 1) + \sum_{i=1}^{j} f_i \,, \tag{1}$$

where j is the number of joints, l is the number of links including the ground, and f_i is the number of constraints for each joint i. For an internally reconfigurable system the wheel is not allowed to translate, but is allowed to rock about two axes in the plane of the terrain and twist about an axis normal to the terrain.

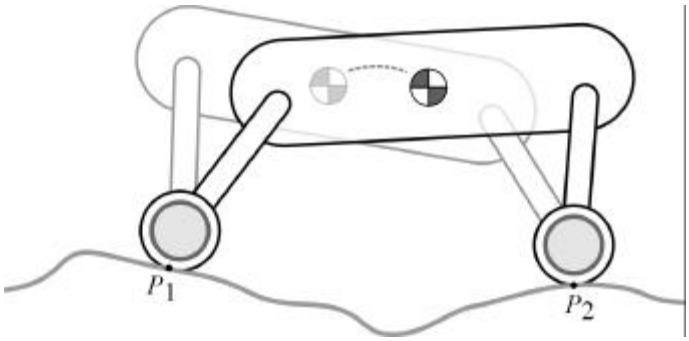

Figure 4. Planar view of an internally reconfigurable mobile robot

For an internally reconfigurable robot the terrain profile does not influence the reconfiguration process. The robot configuration can be defined without terrain information as $Q = (q_1 \ldots q_n, f, c)$. Thus, knowledge of robot kinematics alone is sufficient to pose the optimization problem. Note that for an internally reconfigurable system it is theoretically possible to find a globally optimal solution for the kinematic configuration. The dimension of the optimization search space is equal to the internal mobility F of the system.

Optimization constraints in internally reconfigurable systems take the form of kinematic joint limit and interference constraints, and kinematic loop equations between link-terrain contact points to ensure they remain fixed.

2.2 External reconfigurability

In external reconfigurability the link-terrain contact points P_j move relative to the terrain during the reconfiguration process. The robot in Figure 1 is an example of an externally reconfigurable robot. Note that the mobility analysis of an externally reconfigurable robot is different from that of an internally reconfigurable robot. Wheel-terrain contacts must be treated as higher-order pairs[10].

For externally reconfigurable robots the terrain profile influences the reconfiguration process. Thus, to pose an optimization problem the terrain profile must be known, which is generally not the case. Without knowledge of the terrain profile it is impossible to find a globally optimal solution for the kinematic configuration. However, the local link-terrain contact angles can be estimated [8,9]. The link-terrain contact angle a_j describes the terrain profile in a local region about the point $\mathbf{p}_j$. An optimization problem can therefore be posed with the constraint that the rover configuration change results in only small displacements of the points $\mathbf{p}_j$ with respect to the terrain. Thus, a locally optimal solution for the kinematic configuration can be found.

Optimization constraints in an externally reconfigurable system take the form of kinematic joint limit and interference constraints, and joint excursion limits that restrict the displacements of the points $\mathbf{p}_j$ with respect to the terrain.

3. STABILITY-BASED KINEMATIC RECONFIGURABILITY

In Section 3.1 a previously-proposed stability metric is briefly reviewed[11]. In Section 3.2 a stability-based performance index is proposed, and an optimization method for reconfigurability is outlined.

3.1 Stability definition

We define vehicle stability in a manner similar to that proposed by Papadopoulos and Rey[11]. This definition is briefly reviewed here.

For the general mobile robot shown in Figure 3, m wheel-terrain contact points $\mathbf{p}_i$, $i=\{1,\ldots,m\}$ are numbered in ascending order in a clockwise manner when viewed from above, see Figure 5. The lines joining the terrain-contact points are referred to as tipover axes and denoted $\mathbf{a}_i$, where the i^{th} tipover axis is given by:

$$\mathbf{a}_i = \mathbf{p}_{i+1} - \mathbf{p}_i, \quad i = \{1,\ldots, m\text{-}1\}, \tag{2}$$

$$\mathbf{a}_m = \mathbf{p}_1 - \mathbf{p}_m . \tag{3}$$

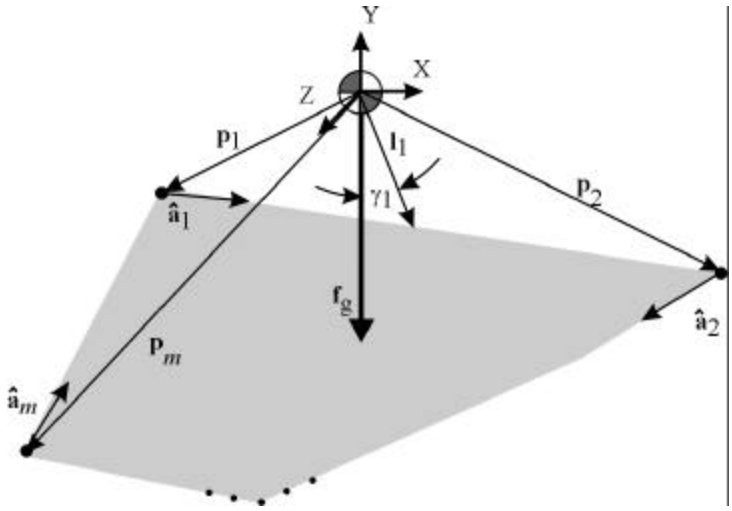

Figure 5. Stability definition diagram

Clearly, a vehicle with m wheels or feet in contact with the terrain has in general m tipover axes.

Tipover axis normals $\mathbf{l}_i$ that intersect the center of mass can be described as:

$$\mathbf{l}_i = \left(\mathbf{1} - \hat{\mathbf{a}}_i \hat{\mathbf{a}}_i^T\right)\mathbf{p}_{i+1}, \tag{4}$$

where $\hat{\mathbf{a}} = \mathbf{a}/\|\mathbf{a}\|$. Stability angles can then be computed for each tipover axis as the angle between the gravitational force vector $\mathbf{f}_g$ and the axis normal $\mathbf{l}_i$:

$$g_i = s_i \cos^{-1}\left(\hat{\mathbf{f}}_g \cdot \hat{\mathbf{l}}_i\right), \quad i = \{1,\ldots,n\}, \tag{5}$$

with

$$s_i = \begin{cases} +1, & \left(\hat{\mathbf{l}}_i \times \hat{\mathbf{f}}_g\right)\cdot \hat{\mathbf{a}}_i < 0 \\ -1, & \text{otherwise} \end{cases}. \tag{6}$$

The overall vehicle stability angle is defined as the minimum of the i stability angles:

$$a = \min(g_i), \quad i = \{1,\ldots,n\}. \tag{7}$$

When $a \le 0$ a tipover instability is occurring. Thus, the goal of stability-based kinematic reconfigurability is to maintain a large value of a.

Note that applied forces, such as those exerted by a manipulator on its environment, can be accounted for in the stability computation. Given an applied force $\mathbf{f}_m$ by the manipulator on its environment, the resultant force along a tipover axis is computed as:

$$\mathbf{f}_i = \left(\mathbf{1} - \hat{\mathbf{a}}_i \hat{\mathbf{a}}_i^T\right)\left(\mathbf{f}_g + \mathbf{f}_m\right). \tag{8}$$

If there is a moment $\mathbf{n}_m$ associated with $\mathbf{f}_m$, the net force about a tipover axis is computed with Equation (8) and:

$$\mathbf{f}_i^* = \mathbf{f}_i + \frac{\hat{\mathbf{l}}_i \times \left(\hat{\mathbf{a}}_i \hat{\mathbf{a}}_i^T\right)\mathbf{n}_m}{\|\mathbf{l}_i\|}, \tag{9}$$

The stability angle a is computed from Equations (5-7) using the net force $\mathbf{f}_i^*$.

3.2 Performance index definition and optimization method description

To optimize the rover configuration for maximum stability, a performance index F is defined based on the stability measure defined in Section 3.1. A function of the following form is proposed:

$$\Phi = \sum_{i=1}^{n}\left(\frac{K_i}{g_i} + K_{n+i}\left(q_i - q_i'\right)^2\right), \tag{10}$$

where g_i are the stability angles defined in Equation (5), q_i are the nominal values of the i^{th} joint variables (i.e. the values of q_i when the robot is at a user-specified configuration), and K_i are constant weighting factors.

The first term of F tends to infinity as the stability at any tipover axis tends to zero. The second term penalizes deviation from a nominal configuration of the shoulder joints, thus maintaining adequate ground clearance, an important consideration in rough terrain. The constants K_i allow control of the relative importance of vehicle stability and joint excursion and therefore ground clearance. Since joint excursion is directly related to power consumption, this can also be viewed as control of the stability-power consumption tradeoff.

The goal of stability-based kinematic reconfigurability optimization problem is to minimize the performance index F subject to joint-limit, interference and possibly kinematic loop constraints. Since F possesses a unique local minimum for simple systems such as the SRR, a rapid optimization technique such as the conjugate-gradient search can be employed[12].

4. SIMULATION RESULTS

Simulation of the JPL SRR traversing rough terrain was performed. The SRR is a 7 kg, four-wheeled mobile robot with independently steered wheels and independently controlled shoulder joints[4]. A 2.25 kg three d.o.f. manipulator is mounted at the front of the SRR. The controllable shoulder joints and manipulator allow the SRR to reposition its center of mass. The SRR is equipped with an inertial navigation system to measure body roll and pitch. Since the ground speed of the SRR is typically 6 cm/sec, dynamic forces do not have a large effect on system behavior, and thus static stability-based reconfigurability is appropriate.

A planar mobility analysis shows that the SRR has a mobility of 0. Thus the rover is only externally reconfigurable. This is intuitively correct, as the SRR cannot reconfigure its shoulder joints without moving wheel-terrain contact points.

The optimization performance index was similar to Equation (10) and considered the two shoulder angle joints q_1 and q_2 and the three manipulator degrees of freedom y_1, y_2, and y_3:

$$\Phi = \sum_{j=1}^{4} \frac{K_j}{g_j} + \sum_{i=1}^{2} K_{i+4} \left(q_i - q_i' \right)^2 . \tag{11}$$

Note that the stability angles g_j are functions of the shoulder and the manipulator degrees of freedom (i.e. $g_j = g_j(q_1, q_2, y_1, y, y_3)$).

Results of a representative simulation trial are shown in Figure 6. Vehicle stability margin as defined by Equation (7) is plotted for reconfigurable and fixed-configuration systems. The mean stability of the reconfigurable system was 37.1% greater than the fixed-configuration system. The stability margin of the fixed-configuration system reaches a minimum value of 1.1°, indicating that the system narrowly avoided tipover failure. The minimum stability margin of the reconfigurable system was 12.5°, a comfortable margin.

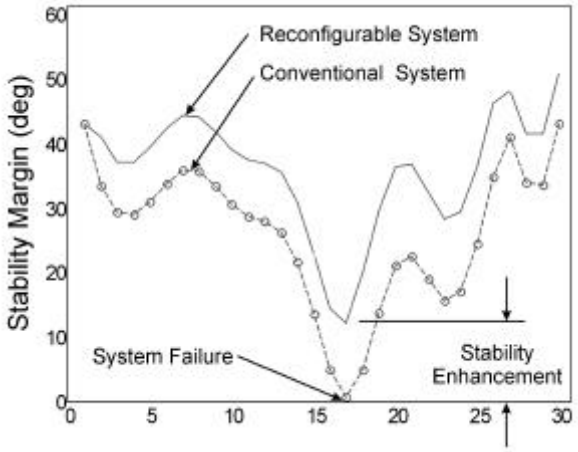

Figure 6. SRR Stability margin for reconfigurable system (solid) and non-reconfigurable system (dashed)

5. EXPERIMENTAL RESULTS

Numerous experimental trials were performed on the SRR in the JPL Planetary Robotics Laboratory and the Arroyo Seco in Altadena, California by a joint MIT/JPL team of researchers. The SRR was commanded to traverse a challenging rough-terrain path that threatened vehicle stability. For each trial the path was traversed first with the shoulder joints fixed, and then with the kinematic reconfigurability algorithm activated.

Results of a representative trial are shown in Figures 7 and 8. Figure 7 shows the shoulder joint angles during the traverse. Both left and right shoulder angles remain within the joint limits of ±45° of the initial values. Note that the non-reconfigurable shoulder angles vary slightly due to servo compliance.

Vehicle stability is plotted for reconfigurable and fixed-configuration traverses in Figure 8. The average stability of the reconfigurable system was 48.1% greater than the fixed-configuration system. The stability margin of the fixed-configuration system reached dangerous minimum values of 2.1° and 2.5°. The minimum stability margin of the reconfigurable system was 15.0°. Clearly, kinematic reconfigurability results in greatly improved stability in rough terrain.

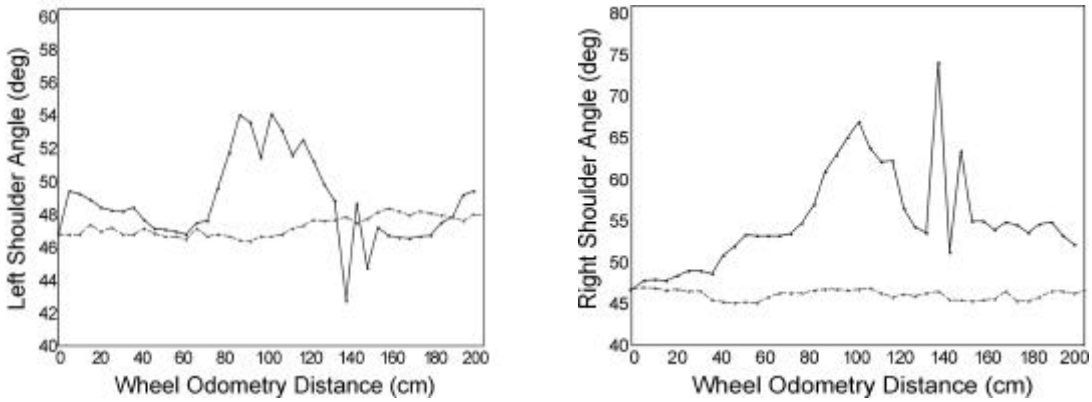

Figure 7. SRR left (a) and right (b) shoulder angles during rough-terrain traverse for reconfigurable system (solid) and non-reconfigurable system (dashed)

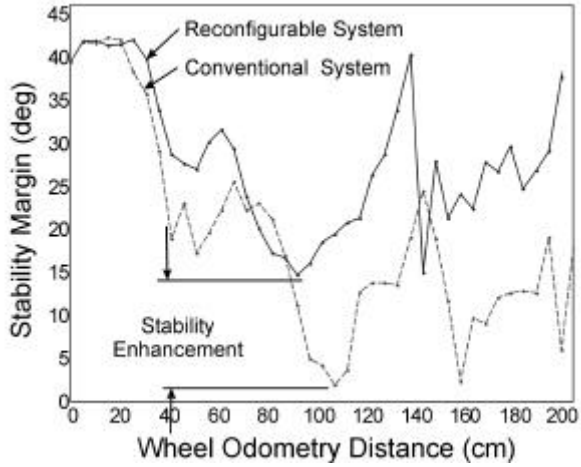

Figure 8. SRR stability margin for reconfigurable system (solid) and non-reconfigurable system (dashed)

Optimization was performed on-line with a 300MHz AMD K6 processor. Average processing time for a single constrained optimization computation was 40 *m*sec. Thus, kinematic reconfigurability of a simple system is feasible for on-board implementation.

6. CONCLUSIONS

A method for stability-based reconfigurability has been presented. The method utilizes kinematic equations relating the reconfigurable joint variables to the vehicle stability angles. A performance index based on these stability angles is optimized subject to vehicle constraints. Simulation and experimental results for the JPL SRR show that the method yields greatly improved vehicle stability in rough terrain.

ACKNOWLEDGMENTS

The assistance of the Planetary Robotics Laboratory staff in conducting experimental trials with the SRR is greatly appreciated. This work is supported by the NASA Jet Propulsion Laboratory under contract number 960456.

REFERENCES

1. M. Golombek, "Mars Pathfinder Mission and Science Results," *Proceedings of the 29th Lunar and Planetary Science Conference*, 1998.
2. S. Hayati, R. Volpe, P. Backes, J. Balaram, and W. Welch, "Microrover Research for Exploration of Mars," *AIAA Forum on Advanced Developments in Space Robotics*, 1998.
3. P. Schenker, L. Sword, A. Ganino, D. Bickler, G. Hickey, D. Brown, E. Baumgartner, L. Matthies, B. Wilcox, T. Balch, H. Aghazarian, and M. Garrett, "Lightweight Rovers for Mars Science Exploration and Sample Return," *Proceedings of SPIE XVI Intelligent Robots and Computer Vision Conference*, **3208**, pp. 24-36, 1997.
4. T. Huntsberger, E. Baumgartner, H. Aghazarian, Y. Cheng, P. Schenker, P. Leger, K. Iagnemma, and S. Dubowsky, "Sensor Fused Autonomous Guidance of a Mobile Robot and Applications to Mars Sample Return Operations," *Proceedings of the SPIE Symposium on Sensor Fusion and Decentralized Control in Robotic Systems II*, **3839**, 1999.
5. S. Sreenivasan, and B. Wilcox, "Stability and Traction Control of an Actively Actuated Micro-Rover," *Journal of Robotic Systems*, **11**, No. 6, pp. 487-502, 1994.
6. S. Sreenivasan, and K. Waldron, "Displacement Analysis of an Actively Articulated Wheeled Vehicle Configuration With Extensions to Motion Planning on Uneven Terrain," *ASME Journal of Mechanical Design*, **118**, No. 2, pp. 312-317, 1996.
7. S. Farritor, H. Hacot, and S. Dubowsky, "Physics-Based Planning for Planetary Exploration," *Proceedings of the 1998 IEEE International Conference on Robotics and Automation*, Belgium, May 1998.
8. K. Iagnemma, and S. Dubowsky, "Vehicle Wheel-Ground Contact Angle Estimation: with Application to Mobile Robot Traction Control," *7th International Symposium on Advances in Robot Kinematics, ARK '00*, pp.137-146, 2000.
9. J. Balaram, "Kinematic State Estimation for a Mars Rover," Accepted for publication in *Robotica, Special issue on Intelligent Autonomous Vehicles*, 2001.
10. H. Eckhardt, *Kinematic Design of Machines and Mechanisms*, McGraw-Hill, New York, 1989.
11. E. Papadopoulos and D. Rey, "A New Measure of Tipover Stability Margin for Mobile Manipulators," *Proceedings of the IEEE International Conference On Robotics and Automation*, 1996.
12. J. Arora, *Introduction to Optimum Design*, McGraw-Hill, New York, 1989.